Published in final edited form as:
Traffic. 2013 June ; 14(6): 709–724. doi:10.1111/tra.12059.

Flotillins regulate membrane mobility of the dopamine transporter but are not required for its protein kinase C dependent endocytosis

Tatiana Sorkina, **John Caltagarone**, and **Alexander Sorkin***
Department of Cell Biology, University of Pittsburgh School of Medicine

SUMMARY

Flotillins were proposed to mediate clathrin-independent endocytosis, and recently, flotillin-1 was implicated in the protein kinase C (PKC)-triggered endocytosis of the dopamine transporter (DAT). Since endocytosis of DAT was previously shown to be clathrin-mediated, we re-examined the role of clathrin coat proteins and flotillin in DAT endocytosis using DAT tagged with the hemagglutinin epitope (HA) in the extracellular loop and a quantitative HA antibody uptake assay. Depletion of flotillin-1, flotillin-2 or both flotillins together by small interfering RNAs (siRNAs) did not inhibit PKC-dependent internalization and degradation of HA-DAT. In contrast, siRNAs to clathrin heavy chain and μ2 subunit of clathrin adaptor complex AP-2 as well as a dynamin inhibitor Dyngo-4A significantly decreased PKC-dependent endocytosis of HA-DAT. Similarly, endocytosis and degradation of DAT that is not epitope-tagged were highly sensitive to the clathrin siRNAs and dynamin inhibition but were not affected by flotillin knockdown. Very little co-localization of DAT with flotillins was observed in cells ectopically expressing DAT and in cultured mouse dopaminergic neurons. Depletion of flotillins increased diffusion rates of HA-DAT in the plasma membrane, suggesting that flotillin-organized microdomains may regulate the lateral mobility of DAT. We propose that clathrin-mediated endocytosis is the major pathway of PKC-dependent internalization of DAT, and that flotillins may modulate functional association of DAT with plasma membrane rafts rather than mediate DAT endocytosis.

Keywords

endocytosis; dopamine transporter; flotillin; clathrin; protein kinase C

INTRODUCTION

Uptake of extracellular macromolecules, viruses and transmembrane proteins residing at the cell surface into cytoplasm is mediated by endocytosis. Endocytosis via clathrin coated pits and vesicles is the major pathway of cargo sorting and internalization (1). Several endocytic mechanisms that do not require clathrin have also been described (2). One of the clathrin-independent pathways has been suggested to involve proteins called flotillins (3). Flotillin-1 (Reggie-2) and flotillin-2 (Reggie-1) are evolutionally conserved and homologous proteins that are associated with the membrane through their palmitoylation and myristoylation, and possibly hydrophobic domains inserted into the bilayer ((4, 5); reviewed in (6) and (7)). Flotillin-1 and -2 form homo- and hetero-oligomers, and are proposed to organize membrane

*Corresponding author: Alexander Sorkin, Department of Cell Biology, University of Pittsburgh, School of Medicine,S368 Biomedical Science Tower, South, 3500 Terrace Street, Pittsburgh, PA 15261, Phone: 412-6243116, FAX: 412-648-8330, sorkin@pitt.edu.

The authors have no conflict of interest to declare.

microdomains, or rafts, enriched in cholesterol, which typically do not contain caveolin and are distinct from caveolae (7, 8). Flotillins are detected in the plasma membrane and various intracellular membrane compartments (9, 10).

The first evidence for the endocytosis-mediating function of flotillins was reported in the study demonstrating flotillin-1 dependent, clathrin-independent endocytosis of glycosylphosphatidyl inositol (GPI)-anchored proteins (3). Subsequent studies produced variety of the data confirming or not confirming the role of flotillins in endocytosis of GPI-anchored proteins and various transmembrane cargo (6, 11–17). In these studies, flotillins were implicated in various types of endocytic mechanisms: both clathrin-and dynamin-dependent, and clathrin- and dynamin-independent. In cases of flotillin's involvement in CME, flotillins were proposed to be upstream of cargo interaction with clathrin coated pits (16, 17). Mouse knockout of flotillin-1 is fertile and healthy, and no defects in endocytosis in flotilin1−/− mice were revealed (18). Importantly, the latter study also showed that no transmembrane proteins were found in flotillin-containing membrane microdomains (18). Altogether these diverse data are difficult to reconcile in one model of the flotillin function, and the role of flotillins in endocytosis remains questionable (7).

Recently, Cremona and co-workers reported that flotillin-1 is necessary for endocytosis of the plasma membrane dopamine transporter (DAT) and glutamate transporter EAA2 (19). One of the key observations in this study was the demonstration that RNAi knock-down of flotillin-1 inhibits PMA-induced PKC-dependent endocytosis of DAT expressed in HEK293 cells. These findings were surprising because it has been previously shown that PKC-dependent endocytosis of DAT requires clathrin and dynamin in several experimental models (20–24). Heterologously-expressed DAT is ubiquitinated in response to PKC activation in several types of cells, and it has been proposed that ubiquitinated DAT is recognized by ubiquitin adaptors in clathrin-coated pits (22, 25, 26). Mutations of DAT ubiquitination sites strongly inhibited PKC-dependent endocytosis (27, 28), as did the knockdown of E3 ubiquitin ligase Nedd4-2 or ubiquitin adaptors (22). Moreover, cholesterol-disrupting compounds did not affect DAT internalization, indicating that cholesterol-rich lipid rafts are not directly involved in DAT endocytosis (21, 23, 29). These apparent discrepancies in the experimental data and a possibility that flotillin-1 may regulate DAT ubiquitination, a step upstream of clathrin coated pit recruitment, prompted us to re-analyze the role of flotillins and clathrin coat components in PKC-dependent endocytosis of DAT. Using epitope-tagged and untagged DATs stably expressed in HEK293 cells we confirmed clathrin-dependence of DAT endocytosis in these cells. In contrast, depletion of flotillin-1 alone or together with flotillin-2 did not decrease PKC-dependent endocytosis of DAT in HEK293 and HeLa cells. Together with the lack of significant co-localization and interaction of flotillins and DAT in cells, the data suggest that flotillins are not essential for PKC-dependent endocytosis of DAT and that DAT is internalized mainly through clathrin coated pits.

RESULTS

siRNAs to flotillin-1 and flotillin-2 do not inhibit PKC-dependentendocytosis of DAT

The role of flotillin-1 in PMA-induced PKC-dependent DAT endocytosis was previously shown in human embryonic kidney HEK293 cells expressing human DAT (19). Hence we used HEK293 cells constitutively expressing human DAT tagged with CFP (cyan fluorescent protein) at the amino-terminus and hemagglutinin epitope (HA11) in the second extracellular loop (HEK/CFP-HA-DAT). These cells allow quantitative single-cell analysis of DAT endocytosis using an HA11 antibody uptake assay (22). As shown in Fig. 1 treatment of HEK/CFP-HA-DAT cells with phorbol ester (PMA) caused dramatic redistribution of the antibody-bound DAT from the cell surface to endosomes. To analyze

the importance of flotillin-1 in DAT endocytosis in these cells, RNAi approach was used. Screening of several siRNA duplexes from different commercial sources identified duplex 6 (D6) from Qiagen, Inc. and SmartPool (SP) from Thermo Fisher Scientific as the most effective in depleting flotillin-1 protein in human cells. Experiments in which flotillin-1 was depleted by at least 70% were used in the immunofluorescence microscopy analysis of CFP-HA-DAT endocytosis.

The HA11 uptake assay demonstrated that PMA triggers robust CFP-HA-DAT endocytosis in cells transfected with flotillin-1 siRNAs (Fig. 1). Staining of the flotillin-1 siRNA transfected cells with flotillin-1 antibody confirmed strong down-regulation of flotillin-1 (Fig. 1A, insets), although cells with residual flotillin-1 were occasionally detected. However, such cellsdid not display increased CFP-HA-DAT endocytosis. For calculations of the endocytosis efficiency in flotillin-1 siRNA treated cells, images with no individual cells exhibiting detectable flotillin-1 staining were exclusively used. Interestingly, in all experiments transfection of cells with flotillin-1 siRNA increased the apparent extent of PMA-induced DAT endocytosis, although this increase was statistically significant only when D6 was used. These data suggest that flotillin-1 is not required for PKC-dependent endocytosis of CFP-HA-DAT.

Flotillin-2 is highly homologous to flotillin-1, and hetero-oligomerization of two flotillins has been implicated in their functions in protein scaffolding and organization of lipid rafts (8). In some cells, where only flotillin-2 is expressed, its function in endocytosis in the absence of flotillin-1 was proposed (17). Therefore, we tested whether flotillin-2 may functionally compensate for the absence of flotillin-1 in promoting DAT endocytosis. However, knockdown of flotillin-2 alone or together with flotillin-1 did not reduce PMA-induced endocytosis of CFP-HA-DAT (Fig. 2A). Interestingly, depletion of flotillin-1 resulted in down-regulation of flotillin-2, and vice versa (Fig. 2B and C), confirming interdependence of both flotillins in regulating their turnover (9, 18, 30).

To assess whether inability to reveal the flotillin function in DAT endocytosis is due to the use of CFP- and HA-tagged DAT, siRNA experiments were performed in HEK 293 cells constitutively expressing untagged DAT (HEK/DAT cells) (Fig. 2C and 3). PMA caused dramatic re-distribution of DAT in HEK293/DAT cells from cell edges (mostly plasma membrane) to intracellular vesicles (endosomes) (Fig. 3). RNAi experiments demonstrated that flotillins are not necessary for accumulation of untagged, wild-type DAT in endosomes upon PMA treatment in this experimental model (Fig. 3). Finally, the effect of flotillin-1 knockdown was tested in another human cellline, HeLa, that stably express YFP (yellow fluorescent protein) and HA-tagged human DAT (YFP-HA-DAT), using an HA11 antibody uptake assay (Fig. 4). No reduction of PMA-induced endocytosis was observed in HeLa cells depleted of flotillin-1. Altogether, siRNA experiments in several cell lines expressing tagged and untagged DAT demonstrated that PKC-dependent endocytosis of DAT is flotillin-independent.

Membrane mobility of DAT is regulated by flotillins

Because DAT is functionally regulated by localization in cholesterol-rich microdomains and/or by interaction with cholesterol (23, 29, 31, 32), we tested whether flotillins influence the dynamics of DAT in the plasma membrane. To this end, FRAP (fluorescence recovery after photobleaching) analysis was used to measure the rates of diffusion and the mobility fractions of plasma membrane CFP-HA-DAT in HEK293 cells. FRAP was performed at 37°C by photobleaching the small area of cell edges or diffusely-fluorescent areas of cells (“flat” plasma membrane) (Fig. 5A). In both types of plasma membrane regions, knock-down of flotillin-1 resulted in a moderate decrease of τ (half-life of fluorescence recovery) values indicative of an increased diffusion mobility of CFP-HA-DAT, and this effect was

slightly more pronounced in cells depleted of both flotillins (Fig. 5B). The mobile fraction of CFP-HA-DAT was not affected by flotillin siRNAs (Fig. 5C). Overexpression of flotillin-1 tagged with YFP increased the mean value of τ measured in cell edges by 16.5% +/−3.9% (S.E.), although this increase did not reach statistical significance ($P = 0.059$; $n>20$ for each cell population; 3 independent experiments). Furthermore, we have previously reported DAT concentration in filopodia and a large pool of immobile DAT in these structures (33). Flotillin depletion did not cause DAT redistribution from filopodia and did not affect lateral diffusion parameters of DAT in filopodia where about 70–80% of DAT was immobile (data not shown). These experiments demonstrate that flotillins and, possibly, flotillin-based membrane rafts regulate the rate of DAT diffusion in non-filopodial areas of the membrane.

Analysis of co-localization and interaction of flotillin-1 and DAT

Flotillins are associated with the plasma membrane; they are also endocytosed themselves in response to phosphorylation by Src family kinases and are present in intracellular membrane compartments (34). Therefore, subcellular localization of flotillin-1 and DAT was compared by immunofluorescence microscopy in HEK/DAT cells. In non-stimulated cells both DAT and flotillin-1 were mostly located in cell edges, ruffles and other plasma membrane regions (Fig. 6A). Substantial amount of flotillin-1 immunofluorescence was also seen in heterogeneous intracellular structures. The pattern of localization of two proteins in the plasma membrane was, however, distinct. For instance, DAT was distributed diffusely along cell edges, whereas flotillin fluorescence was clustered along the same edges, presumably, due to the assembly of flotillins into microdomains/rafts (Fig. 6A, insets). Treatment with PMA leading to accumulation of DAT in endosomes did not visibly change the subcellular distribution of flotillin-1. Very little overlap of DAT and flotillin-1 staining was detected in endosomes (Pearson coefficient (P.c.)= 0.05) (Fig. 6B). Endocytosed DAT was highly co-localized with the marker of early endosomes EEA.1 (P.c. = 0.28), whereas very small amount of flotillin-1 was associated with early endosomes (P.c. = 0.08). These data suggest that the endocytic routes and intracellular localization of internalized DAT and flotillin-1 are different.

Analysis of flotillin-1 localization in primary postnatal mesencephalon cultures derived from HA-DAT knock-in mice revealed punctate flotillin-1 staining of various cells with the morphology of glia and neurons (Fig. 7). HA-DAT was stained using MAB369 antibody to the amino-terminus of DAT after fixation and permeabilization to detect the total pool of HA-DAT and thus identify dopaminergic neurons. Flotillin-1 was detected in the soma and proximal processes but was difficult to detect in distal axonal processes of dopaminergic neurons (Fig. 7).

Analysis of multiple images suggested that the expression level of flotillin-1 is relatively low in dopaminergic neurons as compared to other cells in these culture preparations. Very little, if any, overlap of flotillin-1 puncta with DAT-containing axonal varicosities as well as other DAT-containing structures was observed. Similar results were obtained in neurons stained with HA11 antibody (data not shown). We have been unable to assess the role of flotillin-1 in PKC-dependent endocytosis in postnatal dopaminergic neurons because PMA-induced endocytosis could not be detected in these cultures in our experiments (35).

To test whether a pool of flotillin-1 interacts with DAT, CFP-HA-DAT was immunoprecipitated using HA11 antibody. HEK/CFP-HA-DAT cells were treated with PMA or vehicle, and HA11 immunoprecipitates were probed for the presence of flotillin-1 (Fig. 8A). Small amounts of flotillin-1 were found in HA11-immunoprecipitates; however, similar amounts of flotillin-1 were found in HA11 precipitates from parental (control) HEK293 cells (Fig. 8A and C). The amounts of flotillin-1 found in HA11

immunoprecipitates from parental and CFP-HA-DAT expressing cells in six independent experiments using Triton X-100 or Igepal-based lysis buffers were not statistically different (Fig. 8D). Similar results were obtained in experiments with untagged DAT that was immunoprecipitated from HEK/DAT cells using MAB369 antibody (data not shown). In the same experiments, specific co-precipitation with CFP-HA-DAT of endocytic protein Eps15, a protein known tointeract with DAT (22), was observed (Fig. 8B and C). These data suggest that flotillin-1 does not interact with DAT in cell lysates under conditions of our experiments.

Clathrin-dependency of PMA-induced DAT endocytosis and degradation

We have previously demonstrated that PMA-induced DAT endocytosis is inhibited when clathrin heavy chain (CHC) is depleted by siRNA in porcine aortic endothelial (PAE) and HeLa cells (21, 22). Because clathrin-independent, flotillin-1-dependent mechanism was proposed to mediate DAT endocytosis in HEK293 cells (19), the effect of CHC siRNA knockdown on DAT endocytosis was tested in these cells. Figure 9A–C demonstrates strong inhibition of CFP-HA-DAT endocytosis in CHC-depleted cells. Residual internalization of CFP-HA-DAT in CHC-depleted cells may, at least in part, be due to incomplete CHC depletion in a population of cells. Indeed, inspection of individual cells treated with CHC siRNA revealed residual CFP-HA-DAT endocytosis in cells with increased residual amounts of CHC (data not shown). Furthermore, CHC siRNA experiments with HEK/DAT cells confirmed the importance of clathrin for PKC-dependent endocytosis of untagged DAT (data not shown).

To compare localization of CFP-HA-DAT with clathrin coated pits, HEK/CFP-HA-DAT cells were transfected with the marker of coated pits, β2 subunit of AP-2 tagged with YFP (β2-YFP). A small number of CFP-HA-DAT puncta was co-localized with β2-YFP puncta, indicative of coated pit localization (Fig. 9D). Indirect immunofluorescence was used to demonstrate localization of DAT in clathrin coated pits in HEK/DAT cells (Fig. 9E). The maximal extent of co-localization in both cell lines was detected 15–20 min after PMA stimulation.

Since clathrin is involved in trafficking processes other than internalization, other approaches were utilized to confirm that PKC-dependent endocytosis of DAT requires clathrin coated pits. Transfections of cells with siRNA to theμ2 subunit of plasma membrane clathrin adaptor AP-2 complex was used to down-regulate this complex. Depletion of one subunit prevents assembly of stable complexes between other subunits of AP-2, thus leading to their proteosomal degradation. As shown in Fig. 10A–C, depletion of AP-2 detected using antibodies to the α-adaptin substantiallyreduced CFP-HA-DAT endocytosis. Furthermore, treatment of HEK/CFP-HA-DAT and HEK/DAT cells with the chemical inhibitor of dynamin activity, Dyngo-4A, dramatically decreased the extent of DAT endocytosis (Fig. 10D–E). Cumulatively, functional inhibitory and co-localization analyses indicate that clathrin-mediated endocytosis is the major route of PKC-dependent endocytosis of DAT in HEK293 cells.

We have previously demonstrated that PKC stimulation results in down-regulation of the DAT protein due to its ubiquitination and targeting to lysosomes for degradation (25). Because it is possible that proper sorting of DAT to specific endosomal compartments might be dependent on flotillins, we examined whether depletion of clathrin and flotillins affects PMA-induced DAT degradation. To this end, HEK/DAT cells transfected with various siRNAs were incubated with cycloheximide to inhibit protein synthesis, and incubated with PMA or vehicle for several hours, and the amount of DAT was analyzed by Western blotting. As shown in Fig. 11A, DAT was dramatically down-regulated in PMA-treated both control cells and flotillin-1 siRNA transfected cells, whereas degradation of DAT was

dramatically decreased in cells transfected with CHC siRNA. Furthermore, depletion of flotillin-1 did not affect ubiquitination of DAT (Fig. 11B). As previously reported (26), ubiquitination of DAT was not inhibited in cells depleted of clathrin, indicative that DAT is ubiquitinated prior to recruitment into clathrin-coated pits. Likewise, degradation and ubiquitination of CFP-HA-DAT were not affected by flotillin depletion (data not shown). Finally, Fig. 11C shows that PMA-induced DAT degradation was significantly slowed down in cells depleted of AP-2 (Fig. 11C). Altogether, the data presented in Fig. 11 further confirm the crucial role of clathrin and AP-2 in PMA-induced down-regulation of DAT, and also demonstrate that flotillins are not essential atall steps of PMA-induced trafficking of DAT.

DISCUSSION

We used an RNA interference approach in several cell culture lines to show that depletion of flotillin-1 and -2 proteins does not inhibit PKC-dependent DAT endocytosis. This conclusion was reached by using a single-cell quantitative analysis based on the measurement of the extent of the HA11 antibody endocytosis by 3-D confocal imaging, although the lack of flotillin siRNA effects on DAT endocytosis was clearly evident from the visual inspection of images. These data are in disagreement with the previously reported observations by Cremona and coworkers that flotillin-1 is necessary for PKC-dependent DAT endocytosis in HEK293 cells (19). We do not know the nature of such a discrepancy. The extent of flotillin depletion in our experiments was comparable or higher than that in other studies that investigated the effects of flotillin knock-downs on endocytosis (13, 16, 17). Moreover, multiple analyses of individual cells within the population of siRNA-transfected cells by effective immunofluorescence detection unequivocally demonstrated normal or enhanced DAT endocytosis in cells with undetectable flotillin-1 or -2 as compared to that in cells with residual flotillin staining. Furthermore, absence of inhibitory effects of flotillin depletion on DAT endocytosis was observed in two cell lines obtained from different parental HEK293 cells, as well as in HeLa cells.

In addition, the role of flotillin-1 in DAT endocytosis was proposed on the basis of the observation that flotillin-1 overexpression rescued partial inhibition of DAT endocytosis by the competitive inhibitor for ATP-binding site of PKCs, bis-indolylmaleimade 1, G 6850, and that this effect was dependent on flotillin-1 phosphorylation and palmitoylation (19).In our experiments overexpression of flotillin-1-YFP in HEK/CFP-HA-DAT cells did not counteract the inhibitory effect of 100 nM G 6850 on CFP-HA-DAT endocytosis (Fig. S1, Supplemental Materials). We and others noticed that the levels of two flotillins vary in different cell types (6). For instance, the expression level of flotillin-1 is substantially higher in HEK293 than in PAE cells (data not shown). Therefore, the possibility still remains that the flotillin-dependent endocytosis is characteristic of an EM4 subclone of HEK293cells used by Cremona and co-workers (19).

By contrast, demonstration of the importance of clathrin in PKC-stimulated endocytosis of DAT in heterologous expression systems has been straightforward using both biochemical (surface biotinylation) and single-cell immunofluorescence assays. Clathrin knockdown by siRNA strongly inhibited endosomal accumulation of DAT in PMA-treated HEK293 (Fig. 9), porcine aortic endothelial (PAE) and HeLa cells (21, 22). Depletion of AP-2 also significantly decreased the extent of DAT endocytosis (Fig. 10). Knockdown of dynamin-2 or overexpression of dynamin K44A mutant blocked PMA-induced endocytosis in PAE, HeLa and MDCK cells, as well as the constitutive DAT endocytosis in cultured dopaminergic neurons (20–22, 24). In the present work, acute treatment of cells with the dynamin inhibitor Dyngo-4A also blocked DAT endocytosis (Fig. 10).Requirement of dynamin activity does not formally prove the involvement of CME; however, inhibition of

this endocytic mechanism is typically the major consequence of dynamin-2 inactivation (36). Inhibition of CME by Concavalin A or high sucrose abolished PMA-induced reduction of surface DATs in LLC-PK1 cells (37) and HEK293 cells (24).

A rather small pool of DAT molecules was detected in clathrin coated pits (Fig. 9) as compared to the relative amounts of “classical” CME cargo such as transferrin and EGF receptors. First, for stimulated endocytosis of EGF receptors, the apparent high extent of receptor localization in coated pits is calculated using labeled ligand (38). Calculation of the coated pit pool relative to the total pool of surface receptors (ligand-occupied and unoccupied) yields much lower percent of coated pit localization. Second, it is difficult to synchronize PMA-induced endocytosis of DAT using a low temperature block due to low activity of PKC at subphysiological temperatures. Thirdly, the pool of DAT capable of endocytosis was proposed to be limited due to a very small amount of ubiquitinated DAT relative to the total surface pool of DAT, major accumulation of DAT in filopodia and its plasma membrane retention (33).

Further, DAT turnover experiments confirmed the role of clathrin and AP-2 in the PMA-induced endocytic trafficking of DAT that involves two ubiquitination-dependent processes, internalization and endosomal sorting, and proved independence of DAT endocytosis from flotillins (Fig. 10). It should be emphasized that clathrin- and ubiquitination-dependence of PMA-induced endocytosis was recently demonstrated for two other SCL6 gene family transporters, glycine transporters 1 and 2 (39, 40) as well as for the glutamate EAA2(GLT-1) transporter (41, 42), and cationic amino acid transporter 1 (43), suggesting that these ubiquitin-based mechanisms are a common means of regulation of various transporters by PKC (44, 45).

The 3-D image analysis demonstrated localization of flotillins at the plasma membrane and structures that are presumably located inside the cell (Figs. 6 and 7). Flotillin-1 immunofluorescence signal in the plasma membrane overlapped with that of DAT, although different distribution patterns of two proteins suggest that there is only a small pool of “truly” co-localized flotillin-1 and DAT. That plasma membrane DAT and flotillins are involved in a functional interaction is suggested by the increased mobility rates of DAT in cells depleted of flotillins (Fig. 5). It is possible that DAT association with flotillin-based microdomains reduce DAT mobility rates. Indeed, DAT was shown to be present in flotillin-rich subcellular membrane fractions (19), although multi-step fractionation resulted in the separation of DAT and flotillin into different fractions (29). Furthermore, our data demonstrating absence of DAT co-immunoprecipitation with flotillin-1 argue against the role of direct DAT and flotilin-1 interactions, although the possibility could not be ruled out, that due to a very weak affinity and/or high detergent sensitivity of the association of DAT with flotillins, specific experimental conditions may be necessary for detection of this interaction.

Alternatively, flotillins could be important for the maintenance of the proper cholesterol distribution and an overall microdomain organization of the membrane. Disruption of this organization may increase the mobility of integral membrane proteins like DAT. Interestingly, PKC-stimulated endocytosis of DAT was apparently increased in cells transfected with flotillin siRNA, in particular, in experiments with the highest extent of flotillin depletion. Although depletion of flotillins in these experiments did not change the pattern of constitutive distribution of DAT, increased mobility of DAT may at least in part explain elevated PMA-stimulated DAT endocytosis. In agreement with our observations, recent study describing new R615C DAT mutant revealed an increased constitutive endocytosis of this mutant and reduced ability of this mutant to co-precipitate with flotillin-1, suggesting that flotillin microdomain association of DAT may have the

propensity to retain DAT at the cell surface (46). Another recent study (47) linked DAT C-terminal amino-acid sequences, implicated in negative regulation of DAT endocytosis (48),to the interaction of DAT with Rin (Rit2) in the vicinity of cholera toxin-labeled lipid rafts. Recently, siRNA knockdown of flotillins was reported to result in endocytosis of normally not-endocytosed receptor tyrosine kinase ErbB2, thus supporting the notion of a flotillin function in the plasma membrane stabilization/retention of transmembrane proteins (49)

Flotillin-1 was proposed to be necessary for the DAT-mediated amphetamine-induced efflux of dopamine (19). The behavior effects of amphetamines are dramatically diminished in the absence of flotillin in Drosophila (50). These functional DAT-related effects of flotillin could be attributed to DAT localization in cholesterol-rich membrane microdomains or possibly direct association of DAT with cholesterol, and importance of this localization/interaction for regulation of DAT conformation and function (29, 32). Of note, screening for genes important for endocytosis in Drosophila did not uncover the endocytic function of flotillin (G. D. Gupta and S. Mayor, personal communication).

Endocytosis of flotillins revealed by their accumulation in endosome-like vesicles is triggered by Src family kinases (34). Our experiments suggest that endocytic pathways of flotillin and DAT are different because there is very minimal, if any, co-localization of flotillins and DAT in early endosomes (Fig. 6). This is in agreement with other studies demonstrating that flotillins are not present in conventional early endosomes containing EEA.1 (6, 9). Furthermore, tyrosine kinases appear to have opposite effects on DAT and flotillin endocytosis: DAT endocytosis is either not effected (19) or accelerated by tyrosine kinase inhibitors (51, 52).

In summary, our data do not support the model of flotillin-mediated endocytosis. Despite a number of studies implicating flotillins in endocytosis, the function of flotillins as the core component directly involved in the process of forming the endocytic vesicle from the plasma membrane is not demonstrated (7). Flotillin-1−/− knockout mice are viable and have no apparent phenotypes (18). This lack of phenotype was not due to a compensatory function of flotillin-2 because flotillin-2 was dramatically down-regulated in these animals and did not partition in raft-like microdomains. Further analysis of endocytic processes in cells derived from these flotillin-1 knockouts may shed light on the role of flotillins in endocytosis and other intracellular processes.

MATERIALS AND METHODS

Reagents

Antibodies were purchased from the following sources: monoclonal rat antibody against the N-terminus of DAT (MAB369) from Millipore (Temecula, CA); polyclonal rabbit antibody to ubiquitin from Sigma-Aldrich (St. Louis, MO); mouse monoclonal antibody to hemagglutinin epitope HA11 (16B12) from Covance (Berkley, CA); monoclonal mouse antibody to EEA.1 from BD Biosciences (Franklin Lakes, NJ); antibody to α-subunit of AP-2 AC.1-M11 from (Thermo Fisher Scientific, Pittsburgh, PA, USA); donkey anti-mouse, anti-rat and anti-rabbit antibodies conjugated with Alexa488, Cy5, Cy3 and FITC from Jackson Immuno Research (West Grove, PA); X22 clathrin monoclonal antibody from American Type Cell Culture Collections, Inc. (ATCC) (Manassas, VA); monoclonal mouse antibody to Flotillin-1 from Santa Cruz Biotechnology, Inc. (Santa Cruz, CA); monoclonal rabbit antibody to flotillin-1 and polyclonal rabbit antibody to flotillin-2 from Epitomics (Burlingame, CA) (now Abcam) and polyclonal rabbit antibody to CHC from Abcam (Cambridge, MA).IRDye-800 and IRDye-680-conjugated goat anti-mouse, anti-rat and anti-rabbit antibodies were purchased from LI-COR Biosciences (Lincoln, NE). Transferrin

conjugated with Alexa 488 was purchased from Invitrogen (Grand Island, NY). Protein G-Sepharose was purchased from Invitrogen. siRNAs to Flotillin-1 and Non-Targeting siRNA were purchased from Qiagen (Valencia, CA); siRNAs to CHC and μ2/AP-2 (53) and Smart Pools of duplexes to flotillin-1 and flotillin-2 were purchased from Thermo Fisher Scientific. Dyngo-4A was purchased from Abcam. Paraformaldehyde was from Electron Microscopy Sciences (Hatfield, PA). Tissue culture reagents were purchased from Invitrogen. Phorbol 12-myristate 13-acetate (PMA), Igepal, Triton X-100, protease Inhibitors and most other reagents were purchased from Sigma Aldrich (St. Louis, MO). Bisindolylmaleimide 1 (G6850) was pur chased from EMD Millipore (Billerica, MA).

Cell culture and transfections

Human HEK293T cells were purchased from American Type Cell Culture Collections, Inc. HEK293T cells stably expressing CFP-HA-DAT were described previously (26). HEK293 cells expressing human DAT were generated by cloning in the presence of G418 (400 μg/ml). HeLa stably expressing YFP-HA-DAT were previously described (22). HEK293T and HeLa cells were grown in DMEM containing 10% fetal bovine serum. All cell lines were regularly checked for mycoplasma using Lonza (Allendale, NJ) mycoplasma detection kit. For live imaging cells were grown on collagen-coated glass bottom plates (MatTek, Ashland, MA), and for other experiments on Poly-D-Lysin (Sigma Aldrich) or Entactin-Collagen IV-Laminin Cell Attachment Matrix (Millipore) pre-coated glass coverslips or Falcon plates.

siRNA transfections were performed with DharmaFECT® Transfection Reagent #1 from Thermo Fisher Scientific according to manufacturer's recommendations and as described previously (21, 22). Typically, transfection with siRNAs was repeated after two days, and pooled cells from each control or experimental knockdown were plated for all experimental conditions. Cells were grown two more days and assayed on the fifth day after the first siRNA transfection. In some experiments single transfection with siRNA to CHC was used, and cells were assayed on the third day after transfection. Efficiency of target protein knock-down was determined for each experiment by immunofluorescence assay and/or Western blot.

β2-YFP was previously characterized (54). Flotillin-1-YFP construct was kindly provided by Dr. R. Tikkanen (University of Giessen, Germany). The cells were transfected with plasmids using Effectine kit (Qiagen) by following manufacturer's protocol.

DA neuronal cultures

Primary mesencephalic postnatal cultures were prepared as previously described (35). Experiments were performed on neurons at days *in vitro* (DIV) 6–10.

Antibody uptake endocytosis assay and immunofluorescence detection

The endocytosis assay using HA11 antibody was performed similarly as described in Sorkina, 2006. Briefly, the cells grown on glass coverslips were incubated with 2 μg/ml HA11 in conditioned media (same media the cells were grown) for 30 min and then in DMEM with DMSO (vehicle) or PMA (1 μM), all at 37°C in 5% CO2 atmosphere, for the indicated times. The cells were washed with ice-cold HBSS (Invitrogen) and fixed with freshly prepared 4% paraformaldehyde for 15 min at room temperature. The cells were incubated with secondary donkey anti-mouse antibody conjugated with FITC (fluorescein) or Cy5 (5 μg/ml) in DPBS (Invitrogen) containing 0.5% BSA at room temperature for 1 hr. to occupy surface HA11. After triple wash and additional 15-min fixation, the cells were permeabilized by 5-min incubation in DPBS containing 0.1% Triton X-100/0.5% BSA at room temperature, and then incubated with the same secondary antibody conjugated with

Cy3 (1 μg/ml) in DPBS/0.5% BSA for 45 min to label internalized HA11. Each antibody incubations were followed by a 2-min wash in DPBS/0.5% BSA, repeated three times. Both primary and secondary antibody solutions were precleared by centrifugation at 100,000 × g for 20 min. Coverslips were mounted on slides in Mowiol (Calbiochem, La Jolla, CA).

For conventional immunofluorescence staining, the cells on coverslips were fixed with paraformaldehyde and permeabilized with Triton X-100 as above, incubated with appropriate primary and secondary antibodies, each followed by triple washes, and mounted in Mowiol. In experiments requiring co-staining of rat and mouse-developed antibody, all primary and secondary antibody incubations were performed sequentially, separated by additional fixation.

Fluorescence microscopy

To obtain high resolution three-dimensional (3D) images of the cells, a z-stack of confocal images was acquired using a spinning disk confocal imaging system based on a Zeiss Axio Observer Z1 inverted fluorescence microscope (with 63x Plan Apo PH NA 1.4), equipped with a computer-controlled Spherical Aberration Correction unit, Yokogawa CSU-X1, Vector photomanipulation module, Photometrics Evolve 16-bit EMCCD camera, HQ2 cooled CCD camera, environmental chamber and piezo stage controller and lasers (405, 445, 488, 515, 561, and 640 nm) (Intelligent Imaging Innovations, Inc., Denver, CO), all controlled by SlideBook 5 software (Intelligent Imaging Innovation, Denver, CO). Typically, up to 50 serial two-dimensional confocal images were recorded at 200–300 nm intervals. All image acquisition settings were identical in each experiment.

Quantification of the relative amount of Cy5 or FITC (surface) and Cy3 (internalized) fluorescence was performed using the statistics module of the SlideBook5. The background-subtracted 3D images were segmented using a minimal intensity of Cy5 or FITC (non-permeabilized cells staining) and Cy3 (permeabilized cells staining) as a low threshold to obtain segment masks #1 and 2, respectively, corresponding to the total amount of surface and intracellular HA11, correspondingly. Additionally, segment mask #3 of Cy3 fluorescence overlapping with Cy5/FITC positive pixels was generated to determine the amount of Cy3-labeled antibodies that bind to surface HA11 due to incomplete occupancy of surface HA11 with Cy5/FITC-labeled secondary antibodies before cell permeabilization. Mask #3 was subtracted from Mask #2 to obtain Mask #4 corresponding to the corrected Cy3 fluorescence (internalized HA11 complexes with YFP- or CFP-HA-DAT). The integrated voxel intensity of Masks #1 and #4 were quantitated in each image containing typically 5–15 cells, and the ratio of Mask#4 to Mask#1 integrated intensities were calculated to determine the extent of DAT internalization.

Fluorescence Recovery after Photobleaching (FRAP)

HEK/CFP-HA-DAT cells were grown on glass bottom MatTek dishes.FRAP measurements were carried out in growth medium at 37°C. FRAP experiments were performed using a spinning disk confocal microscope system equipped with an environmental chamber ensuring a constant temperature, humidity and 5% CO2 atmosphere throughout the duration of the imaging. Time-lapse imaging was conducted via a 63X objective lens using a 445 nm laser line before and after photobleaching through Vector photomanipulation module at 488 nm. Each experiment started with a minimum of 4 pre-bleach images, followed by photobleaching using 3x3 μm-rectangles of different regions of cells. Images were obtained using 100–150 ms exposure times with 1 s intervals for a total of 100 s. Recovery curves were plotted, and mobility fractions (Mf) and diffusion half-life times (τ) were calculated using SlideBook5 FRAP module. Under each experimental condition, FRAP was measured in 15–20 cells.

Immunoprecipitation

In co-immunoprecipitation experiments cells grown in 100 mm dishes were incubated with 1 μM PMA or vehicle for 15 or30 min at 37°C in 5% CO2 atmosphere, washed with ice-cold DPBS, and the proteins were solubilized in TGH (1%Triton X-100, 10% glycerol, 20 mM HEPES, 50 mM NaCl) or IGH (0.8% Igepal, 0.2% Triton X-100, 5% Glycerol, 20 mM HEPES, 50 mM NaCl) lysis buffer supplemented with 10 mM N-ethyl maleimide (NEM) (inhibitor of deubiquitination) and protease and phosphatase inhibitors for 30–60 min at 4°C. Lysates were centrifuged at 100,000 × g for 20 min to remove insoluble material, and then precleared with 120 μl Protein G-Sepharose for 1 hour, followed by 3 min centrifugation at 21000 × g. All procedures were done at 4°C. Aliquots (5%) of precleared lysates were taken for input control. Lysates were then incubated with 12 μg of mHA11 or MAB369 antibodies overnight and protein-antibody complexes were precipitated with Protein G-Sepharose for 1 hr., followed by two washes in lysis buffer containing 100 mM NaCl and one wash without NaCl. All incubations were done at 4°C with gentle rotation on nutator. Immunoprecipitates and aliquots of cell lysates were denatured in sample buffer for 5 min at 95°C, resolved by SDS-PAGE, transferred to nitrocellulose and probed with appropriate primary and secondary antibodies conjugated to far-red fluorescent dyes (IRDye-680 and -800) followed by detection using Odyssey Li-COR system. Quantifications were performed using Li-COR software.

To analyze DAT ubiquitination, cells grown in 12-well plates were incubated with PMA or vehicle for 30 min at 37°C in 5% CO2 atmosphere, solubilized in TGH containing 1% sodium deoxycholate, 10 mM dithiothreitol, 10 mM NEM and protease and phosphatase inhibitors for 30 min at 4°C and centrifuged at 21000 × g for 10 min to remove insoluble material. Lysates were incubated with appropriate (MAB369 or HA11) antibodies overnight followed by Protein G-Sepharose for 1 hour at 4°C and processed as described above for protein detection by Western blotting.

Degradation experiments

HEK/DAT cells were sequentially transfected twice with appropriate siRNAs and plated onto 12-well plates. On the fifth day after initial SiRNA transfection confluent cells were incubated with 50 μM cycloheximide (CHX) at 37°C for 2 hours, followed by incubation with DMSO (vehicle) or 1 μM PMA in DMEM for indicated times at 37°C in 5% CO2 atmosphere, washed with cold DPBS and solubilized in TGH containing 1% sodium deoxycholate and protease inhibitors for 60 min at 4°C. The lysates were subjected to SDS-PAGE and Western blotting as described above.

Statistical analysis

Statistical significance (P value) was calculated using unpaired two-tailed Student’s t tests (Prism 5 and Excel).

Supplementary Material

Refer to Web version on PubMed Central for supplementary material.

Acknowledgments

We thank Dr. R. Tikkanen for generous gift of flotillin-1-YFP, and Dr. Jitu Major for discussion of our data and communication of unpublished results. This work was supported by NIH/NIDA grants DA014204 (T.S., A.S.) and T32DA031111 (J. M. C.).

The abbreviations used are

CME	clathrin-mediated endocytosis
CHC	clathrin heavy chain
CHX	cycloheximide
DAT	dopamine transporter
EGFR	epidermal growth factor receptor
CFP and YFP	cyan and yellow fluorescent protein
PKC	protein kinase C
RNAi	RNA interference
siRNA	small interfering RNA

References

1. McMahon HT, Boucrot E. Molecular mechanism and physiological functions of clathrin-mediated endocytosis. Nature Rev Mol Cell Biol. 2011; 12(8):517–533. [PubMed: 21779028]
2. Howes MT, Mayor S, Parton RG. Molecules, mechanisms, and cellular roles of clathrin-independent endocytosis. Curr Opin Cell Biol. 2010; 22(4):519–527. [PubMed: 20439156]
3. Glebov OO, Bright NA, Nichols BJ. Flotillin-1 defines a clathrin-independent endocytic pathway in mammalian cells. Nat Cell Biol. 2006; 8(1):46–54. [PubMed: 16341206]
4. Babuke T, Tikkanen R. Dissecting the molecular function of reggie/flotillin proteins. Eur J Cell Biol. 2007; 86(9):525–532. [PubMed: 17482313]
5. Neumann-Giesen C, Falkenbach B, Beicht P, Claasen S, Luers G, Stuermer CA, Herzog V, Tikkanen R. Membrane and raft association of reggie-1/flotillin-2: role of myristoylation, palmitoylation and oligomerization and induction of filopodia by overexpression. Biochem J. 2004; 378(Pt 2):509–518. [PubMed: 14599293]
6. Stuermer CA. Reggie/flotillin and the targeted delivery of cargo. J Neurochem. 2011; 116(5):708–713. [PubMed: 21214550]
7. Otto GP, Nichols BJ. The roles of flotillin microdomains--endocytosis and beyond. J Cell Sci. 2011; 124(Pt 23):3933–3940. [PubMed: 22194304]
8. Frick M, Bright NA, Riento K, Bray A, Merrified C, Nichols BJ. Coassembly of flotillins induces formation of membrane microdomains, membrane curvature, and vesicle budding. Curr Biol. 2007; 17(13):1151–1156. [PubMed: 17600709]
9. Langhorst MF, Reuter A, Jaeger FA, Wippich FM, Luxenhofer G, Plattner H, Stuermer CA. Trafficking of the microdomain scaffolding protein reggie-1/flotillin-2. Eur J Cell Biol. 2008; 87(4): 211–226. [PubMed: 18237819]
10. Stuermer CA, Lang DM, Kirsch F, Wiechers M, Deininger SO, Plattner H. Glycosylphosphatidyl inositol-anchored proteins and fyn kinase assemble in noncaveolar plasma membrane microdomains defined by reggie-1 and -2. Mol Biol Cell. 2001; 12(10):3031–3045. [PubMed: 11598189]
11. Gregory AD, Hale P, Perlmutter DH, Houghton AM. Clathrin pit-mediated endocytosis of neutrophil elastase and cathepsin G by cancer cells. J Biol Chem. 2012
12. Neumann-Giesen C, Fernow I, Amaddii M, Tikkanen R. Role of EGF-induced tyrosine phosphorylation of reggie-1/flotillin-2 in cell spreading and signaling to the actin cytoskeleton. J Cell Sci. 2007; 120(Pt 3):395–406. [PubMed: 17213334]
13. Ait-Slimane T, Galmes R, Trugnan G, Maurice M. Basolateral internalization of GPI-anchored proteins occurs via a clathrin-independent flotillin-dependent pathway in polarized hepatic cells. Mol Biol Cell. 2009; 20(17):3792–3800. [PubMed: 19605558]

14. Haugsten EM, Zakrzewska M, Brech A, Pust S, Olsnes S, Sandvig K, Wesche J. Clathrin- and dynamin-independent endocytosis of FGFR3--implications for signalling. PloS One. 2011; 6(7):e21708. [PubMed: 21779335]

15. Carcea I, Ma'ayan A, Mesias R, Sepulveda B, Salton SR, Benson DL. Flotillin-mediated endocytic events dictate cell type-specific responses to semaphorin 3A. J Neurosci. 2010; 30(45):15317–15329. [PubMed: 21068336]

16. Ge L, Qi W, Wang LJ, Miao HH, Qu YX, Li BL, Song BL. Flotillins play an essential role in Niemann-Pick C1-like 1-mediated cholesterol uptake. Proc Natl Acad Sci U S A. 2011; 108(2): 551–556. [PubMed: 21187433]

17. Schneider A, Rajendran L, Honsho M, Gralle M, Donnert G, Wouters F, Hell SW, Simons M. Flotillin-dependent clustering of the amyloid precursor protein regulates its endocytosis and amyloidogenic processing in neurons. J Neurosci. 2008; 28(11):2874–2882. [PubMed: 18337418]

18. Ludwig A, Otto GP, Riento K, Hams E, Fallon PG, Nichols BJ. Flotillin microdomains interact with the cortical cytoskeleton to control uropod formation and neutrophil recruitment. J Cell Biol. 2010; 191(4):771–781. [PubMed: 21059848]

19. Cremona ML, Matthies HJ, Pau K, Bowton E, Speed N, Lute BJ, Anderson M, Sen N, Robertson SD, Vaughan RA, Rothman JE, Galli A, Javitch JA, Yamamoto A. Flotillin-1 is essential for PKC-triggered endocytosis and membrane microdomain localization of DAT. Nat Neurosci. 2011; 14(4):469–477. [PubMed: 21399631]

20. Daniels GM, Amara SG. Regulated Trafficking of the Human Dopamine Transporter. Clathrin-mediated internalization and lysosomal degradation in reponse to phorbol esters. J Biol Chem. 1999; 274(50):35794–35801. [PubMed: 10585462]

21. Sorkina T, Hoover BR, Zahniser NR, Sorkin A. Constitutive and protein kinase C-induced internalization of the dopamine transporter is mediated by a clathrin-dependent mechanism. Traffic. 2005; 6(2):157–170. [PubMed: 15634215]

22. Sorkina T, Miranda M, Dionne KR, Hoover BR, Zahniser NR, Sorkin A. RNA interference screen reveals an essential role of Nedd4-2 in dopamine transporter ubiquitination and endocytosis. J Neurosci. 2006; 26(31):8195–8205. [PubMed: 16885233]

23. Foster JD, Adkins SD, Lever JR, Vaughan RA. Phorbol ester induced trafficking-independent regulation and enhanced phosphorylation of the dopamine transporter associated with membrane rafts and cholesterol. J Neurochem. 2008; 105(5):1683–1699. [PubMed: 18248623]

24. Eriksen J, Rasmussen SG, Rasmussen TN, Vaegter CB, Cha JH, Zou MF, Newman AH, Gether U. Visualization of dopamine transporter trafficking in live neurons by use of fluorescent cocaine analogs. J Neurosci. 2009; 29(21):6794–6808. [PubMed: 19474307]

25. Miranda M, Wu CC, Sorkina T, Korstjens DR, Sorkin A. Enhanced ubiquitylation and accelerated degradation of the dopamine transporter mediated by protein kinase C. J Biol Chem. 2005; 280(42):35617–35624. [PubMed: 16109712]

26. Vina-Vilaseca A, Sorkin A. Lysine 63-linked polyubiquitination of the dopamine transporter requires WW3 and WW4 domains of Nedd4-2 and UBE2D ubiquitin-conjugating enzymes. J Biol Chem. 2010; 285(10):7645–7656. [PubMed: 20051513]

27. Miranda M, Dionne KR, Sorkina T, Sorkin A. Three Ubiquitin Conjugation Sites in the Amino Terminus of the Dopamine Transporter Mediate Protein Kinase C-dependent Endocytosis of the Transporter. Mol Biol Cell. 2007; 18(1):313–323. [PubMed: 17079728]

28. Mortensen OV, Larsen MB, Prasad BM, Amara SG. Genetic Complementation Screen Identifies a Map Kinase Phosphatase, MKP3, as a Regulator of Dopamine Transporter Trafficking. Mol Biol Cell. 2008

29. Hong WC, Amara SG. Membrane cholesterol modulates the outward facing conformation of the dopamine transporter and alters cocaine binding. J Biol Chem. 2010; 285(42):32616–32626. [PubMed: 20688912]

30. Babuke T, Ruonala M, Meister M, Amaddii M, Genzler C, Esposito A, Tikkanen R. Hetero-oligomerization of reggie-1/flotillin-2 and reggie-2/flotillin-1 is required for their endocytosis. Cell Signal. 2009; 21(8):1287–1297. [PubMed: 19318123]

31. Adkins EM, Samuvel DJ, Fog JU, Eriksen J, Jayanthi LD, Vaegter CB, Ramamoorthy S, Gether U. Membrane mobility and microdomain association of the dopamine transporter studied with

fluorescence correlation spectroscopy and fluorescence recovery after photobleaching. Biochemistry. 2007; 46(37):10484–10497. [PubMed: 17711354]

32. Jones KT, Zhen J, Reith ME. Importance of cholesterol in dopamine transporter function. J Neurochem. 2012
33. Sorkina T, Richards TL, Rao A, Zahniser NR, Sorkin A. Negative regulation of dopamine transporter endocytosis by membrane-proximal N-terminal residues. J Neurosci. 2009; 29(5): 1361–1374. [PubMed: 19193883]
34. Riento K, Frick M, Schafer I, Nichols BJ. Endocytosis of flotillin-1 and flotillin-2 is regulated by Fyn kinase. J Cell Sci. 2009; 122(Pt 7):912–918. [PubMed: 19258392]
35. Rao A, Simmons D, Sorkin A. Differential subcellular distribution of endosomal compartments and the dopamine transporter in dopaminergic neurons. Mol Cell Neurosci. 2010
36. Liu YW, Surka MC, Schroeter T, Lukiyanchuk V, Schmid SL. Isoform and splice-variant specific functions of dynamin-2 revealed by analysis of conditional knockout cells. Mol Biol Cell. 2008; 19(12):5347–5359. [PubMed: 18923138]
37. Foster JD, Vaughan RA. Palmitoylation controls dopamine transporter kinetics, degradation, and protein kinase C-dependent regulation. J Biol Chem. 2011; 286(7):5175–5186. [PubMed: 21118819]
38. Sorkina T, Huang F, Beguinot L, Sorkin A. Effect of tyrosine kinase inhibitors on clathrin-coated pit recruitment and internalization of epidermal growth factor receptor. J Biol Chem. 2002; 277(30):27433–27441. [PubMed: 12021271]
39. Fernandez-Sanchez E, Martinez-Villarreal J, Gimenez C, Zafra F. Constitutive and regulated endocytosis of the glycine transporter GLYT1b is controlled by ubiquitination. J Biol Chem. 2009; 284(29):19482–19492. [PubMed: 19473961]
40. de Juan-Sanz J, Zafra F, Lopez-Corcuera B, Aragon C. Endocytosis of the neuronal glycine transporter GLYT2: role of membrane rafts and protein kinase C-dependent ubiquitination. Traffic. 2011; 12(12):1850–1867. [PubMed: 21910806]
41. Susarla BT, Robinson MB. Internalization and degradation of the glutamate transporter GLT-1 in response to phorbol ester. Neurochem Int. 2008; 52(4–5):709–722. [PubMed: 17919781]
42. Garcia-Tardon N, Gonzalez-Gonzalez IM, Martinez-Villarreal J, Fernandez-Sanchez E, Gimenez C, Zafra F. Protein kinase C (PKC)-promoted endocytosis of glutamate transporter GLT-1 requires ubiquitin ligase Nedd4-2-dependent ubiquitination but not phosphorylation. J Biol Chem. 2012; 287(23):19177–19187. [PubMed: 22505712]
43. Vina-Vilaseca A, Bender-Sigel J, Sorkina T, Closs EI, Sorkin A. Protein kinase C-dependent ubiquitination and clathrin-mediated endocytosis of the cationic amino acid transporter CAT-1. J Biol Chem. 2011; 286(10):8697–8706. [PubMed: 21212261]
44. Miranda M, Sorkin A. Regulation of receptors and transporters by ubiquitination: new insights into surprisingly similar mechanisms. Mol Interv. 2007; 7(3):157–167. [PubMed: 17609522]
45. Rotin D, Kumar S. Physiological functions of the HECT family of ubiquitin ligases. Nat Rev Mol Cell Biol. 2009; 10(6):398–409. [PubMed: 19436320]
46. Sakrikar D, Mazei-Robison MS, Mergy MA, Richtand NW, Han Q, Hamilton PJ, Bowton E, Galli A, Veenstra-Vanderweele J, Gill M, Blakely RD. Attention deficit/hyperactivity disorder-derived coding variation in the dopamine transporter disrupts microdomain targeting and trafficking regulation. J Neurosci. 2012; 32(16):5385–5397. [PubMed: 22514303]
47. Navaroli DM, Stevens ZH, Uzelac Z, Gabriel L, King MJ, Lifshitz LM, Sitte HH, Melikian HE. The plasma membrane-associated GTPase Rin interacts with the dopamine transporter and is required for protein kinase C-regulated dopamine transporter trafficking. J Neurosci. 2011; 31(39): 13758–13770. [PubMed: 21957239]
48. Boudanova E, Navaroli DM, Stevens Z, Melikian HE. Dopamine transporter endocytic determinants: carboxy terminal residues critical for basal and PKC-stimulated internalization. Mol Cell Neurosci. 2008; 39(2):211–217. [PubMed: 18638559]
49. Pust S, Klokk TI, Musa N, Jenstad M, Risberg B, Erikstein B, Tcatchoff L, Liestol K, Danielsen HE, van Deurs B, Sandvig K. Flotillins as regulators of ErbB2 levels in breast cancer. Oncogene. 2012

50. Pizzo AB, Karam CS, Zhang Y, Yano H, Freyberg RJ, Karam DS, Freyberg Z, Yamamoto A, McCabe BD, Javitch JA. The membrane raft protein Flotillin-1 is essential in dopamine neurons for amphetamine-induced behavior in Drosophila. Mol Psychiatry. 2012

51. Simon JR, Bare DJ, Ghetti B, Richter JA. A possible role for tyrosine kinases in the regulation of the neuronal dopamine transporter in mouse striatum. Neurosci Lett. 1997; 224(3):201–205. [PubMed: 9131671]

52. Hoover BR, Everett CV, Sorkin A, Zahniser NR. Rapid regulation of dopamine transporters by tyrosine kinases in rat neuronal preparations. J Neurochem. 2007; 101(5):1258–1271. [PubMed: 17419806]

53. Huang F, Khvorova A, Marshall W, Sorkin A. Analysis of clathrin-mediated endocytosis of epidermal growth factor receptor by RNA interference. J Biol Chem. 2004; 279(16):16657–16661. [PubMed: 14985334]

54. Huang F, Jiang X, Sorkin A. Tyrosine phosphorylation of the beta2 subunit of clathrin adaptor complex AP-2 reveals the role of a dileucine motif in the epidermal growth factor receptor trafficking. J Biol Chem. 2003; 278(44):43411–43417. [PubMed: 12900408]

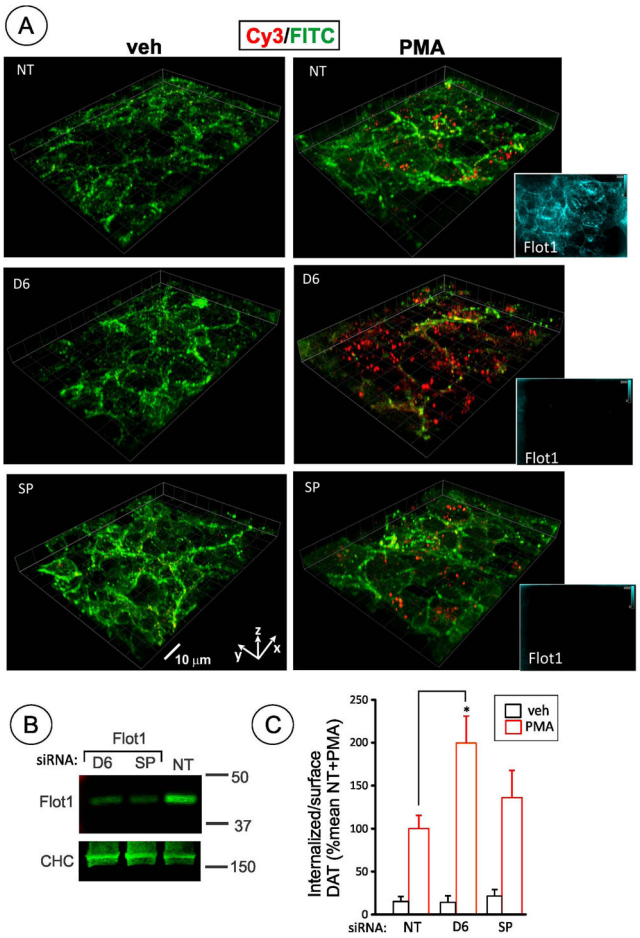

Figure 1. Flotillin-1 siRNA does not inhibit PMA-dependent endocytosis of DAT in HEK293 cells

(**A**) HEK293 cells stably expressing CFP-HA-DAT (HEK/CFP-HA-DAT) were transfected with non-targeting siRNA (***NT***), SmartPool™ (***SP***), or Duplex 6 (***D6***)–both targeting human flotillin-1. Cells were treated with 1 μM PMA or DMSO (***veh***) for 30 min. HA11 internalization assay was performed as described in "Methods". 3D stack of confocal images are presented as merged 3D-volume view images of fluorescein immunofluorescence (green, surface CFP-HA-DAT) and Cy3 immunofluorescence (red, internalized CFP-HA-DAT). In addition to HA11 staining, permeabilized cells were stained with rabbit flotillin-1 antibody followed by secondary conjugated with Cy5 (images are shown in insets on the right). Identical fluorescein, Cy3 and Cy5 (shown) fluorescence intensity scales are used. Scale bars, 10 μM.

(**B**) Western blot detection of flotilin-1 in cells treated as in ***A***. Total cell lysates were blotted with antibodies to flotillin-1 and clathrin heavy chain (CHC) (loading control).The extent of flotillin-1 knockdown by D6 and SP was 90.8% and 81.4% in the experiment presented in (***A***).

(**C**) Quantification of several experiments performed identically to the experiment presented in (***A***). Bars represent the mean values (+/−S.E.) of internalize/surface ratio of HA11-DAT fluorescence normalized to this ratio in control (NT) cells treated with PMA. n=10. *P<0.05.

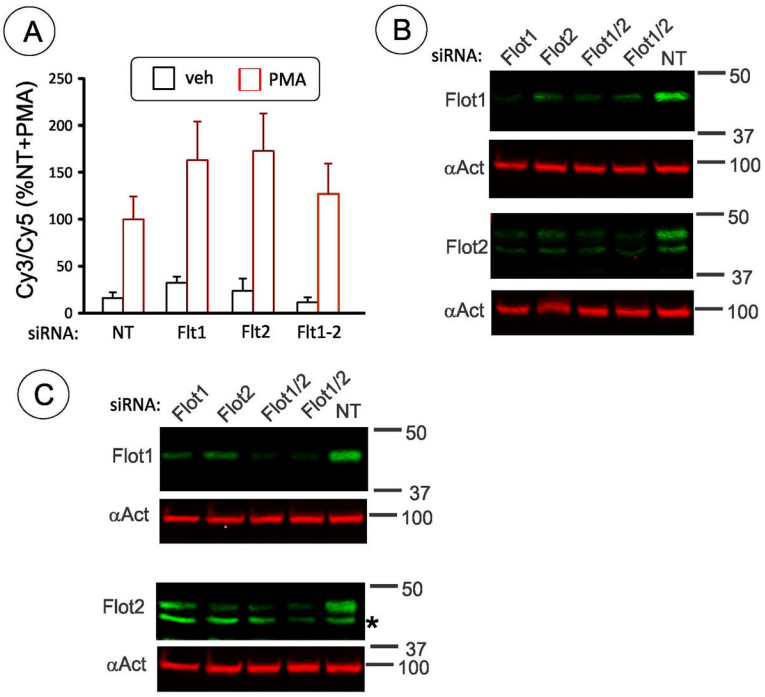

Figure 2. Depletion of both flotillin-1 and flotillin-2 does not inhibit PMA-dependent endocytosis of DAT in HEK293 cells

(**A**) Summary of quantification of several experiments performed as in Fig. 1. HEK/CFP-HA-DAT cells were transfected with non-targeting siRNA (***NT***), SmartPool™ (***SP***) to flotillin-2, siRNA to flotillin-1 (D6 or SP) or together flotillin-1 (D6) and flotillin-2 (SP). Cells were treated with 1 μM PMA or DMSO (***veh***) for 30 min. HA11 internalization assay was performed as described in "Methods" with Cy5 and Cy3 conjugated secondary antibodies detecting, respectively, surface and internalized HA11: CFP-HA-DAT complexes. Bars represent the mean values (+/−S.E.) of internalized/surface ratio (%) of HA11-DAT fluorescence normalized to this ratio in control (NT) cells treated with PMA. **(B**) Representative example of western blot detection of flotilin-1 and flotillin-2 in HEK/CFP-HA-DAT cells treated as in ***A***. Total cell lysates were equally divided and resolved on two parallel gels, then separately blotted with antibodies to flotillin-1, flotillin-2 and α-actinin (loading control). Flotillins were depleted on average by 73.4% in experiments presented in (A).

(C) Representative example of western blot detection of flotilin-1 and flotillin-2 in HEK/DAT cells expressing untagged DAT (HEK/DAT) cells treated as in ***A***. Total cell lysates were equally divided and resolved on two parallel gels, then separately blotted with antibodies to flotillin-1, flotillin-2 and α-actinin (loading control). Cells from the same transfection were used in parallel experiment shown in Figure 3 with average depletion of flotillins by 76.5%.

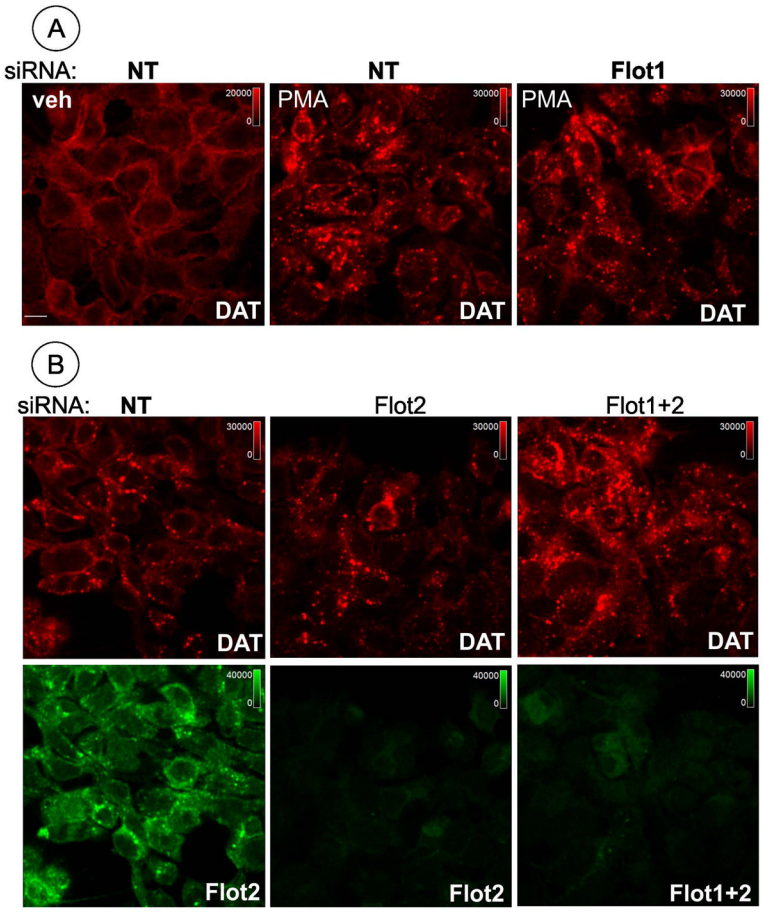

Figure 3. Depletion of flotillin-1 and flotillin-2 does not inhibit PMA-dependent endocytosis of DAT in HEK/DAT cells

HEK/DAT cells were transfected with non-targeting siRNA (***NT***), SmartPool™ (***SP***) to flotillin-2 (**B**), Duplex 6 (D6) (**A**) or together flotillin-1 (D6) and flotillin-2 (SP) (**B**). Cells were treated with 1 μM PMA or DMSO (***veh***) for 30 min. The cells were fixed, permeabilized and stained with rat monoclonal antibody to DAT (red) and rabbit antibodies to flotillin-1 (**A**) or flotillin-2, or both flotillins together (**B**). Representative images (single confocal sections) of 3D stack of confocal images are presented. Identical intensity scales are used and shown on the images. Scale bars, 10 μM.

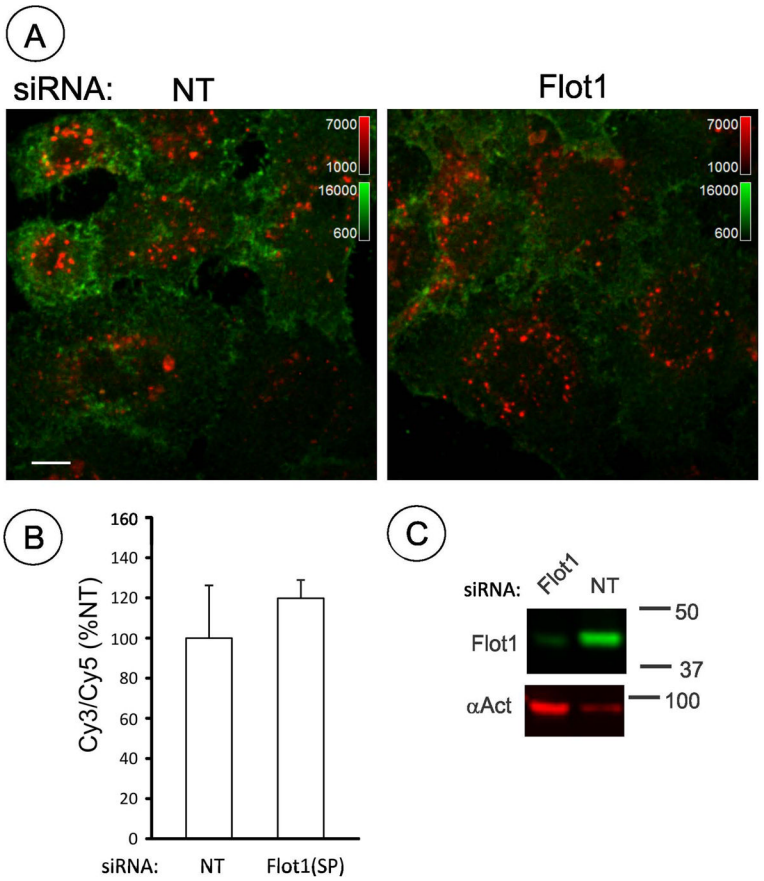

Figure 4. Flotillin-1 siRNA does not inhibit PMA-dependent endocytosis of DAT in HeLa cells

(**A**) HeLa cells stably expressing YFP-HA-DAT (HeLa/YFP-HA-DAT) were transfected with non-targeting siRNA (***NT***) or SmartPool (***SP***) targeting human flotillin-1. Cells were treated with 1 μM PMA or DMSO (***veh***) for 30 min. HA11 internalization assay was performed as described in "Methods". Representative images (single confocal sections) of 3D stack of confocal images are presented. Cy5 immunofluorescence (green, surface YFP-HA-DAT) and Cy3 immunofluorescence (red, internalized YFP-HA-DAT). Identical intensity scales are used. Scale bars, 10 μM.

(**B**) Quantification of several experiments performed identically to the experiment presented in (***A***). Bars represent the mean values (+/−S.E.) of internalized/surface ratio of HA11-DAT fluorescence normalized to this ratio in control (NT) cells treated with PMA.

(C) Western blot detection of flotilin-1 in HeLa/YFP-HA-DAT cells transfected with siRNAs and assayed in parallel as in ***A***. Total cell lysates were blotted with antibodies to flotillin-1 and α-actinin (loading control).

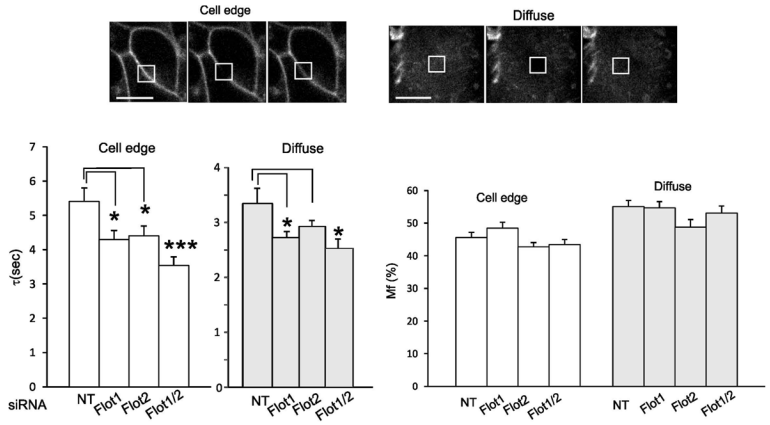

Figure 5. Flotillin depletion increases diffusion mobility rates of CFP-HA-DAT

HEK/CFP-HA-DAT cells were transfected with NT siRNA, siRNAs to flotillin-1 alone or together with flotillin-2 siRNA as in Figure 2. Average depletion of flotillin-1 was 72.8% and 85,2% in single and double siRNA transfected cells. FRAP experiments were performed as described in "Methods".

(A) Examples of images of the CFP fluorescence with focusing on cell edges and on areas of diffuse fluorescence acquired before (-1 s), immediately after (0 s) and 5 sec after photobleaching of the indicated areas.

(**B**) Bar graphs represent mean values of τ and Mf from multiple cells in 3 experiments. S.E. (statistical error); n=16–20. *P<0.05; **P<0.005.

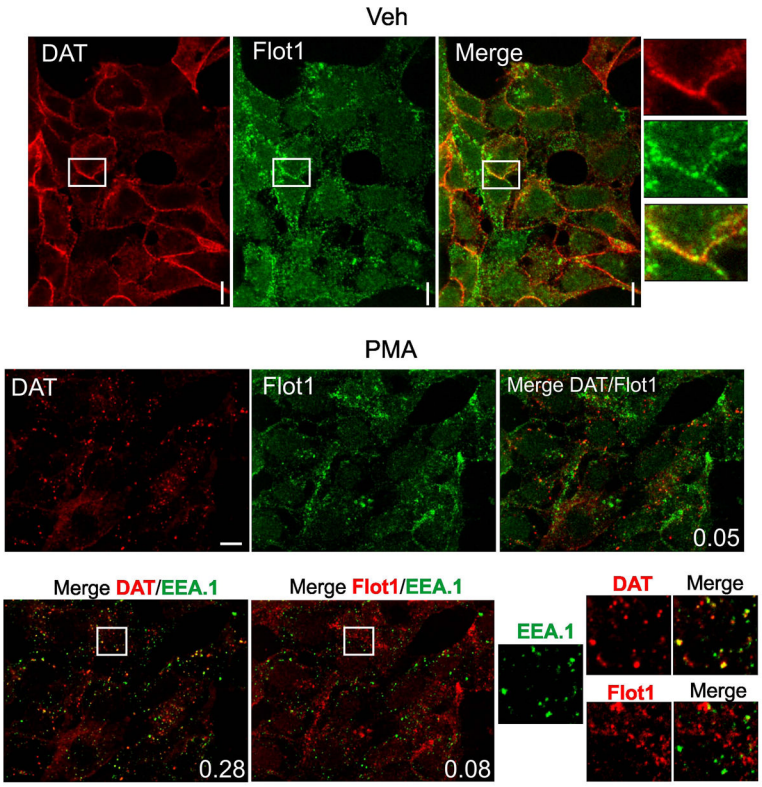

Figure 6. Comparison of localization of flotillin-1 and DAT in HEK293 cells

HEK/DAT cells were treated with 1 μM PMA (B) or DMSO (vehicle) (A) for 30 min. The cells were fixed, permeabilized and stained with rat monoclonal antibody to DAT (red) and rabbit monoclonal antibody to flotillin-1 (green, or red in lower panel) followed by secondary antibodies to rat and rabbit conjugated with Cy3 and Cy5, respectively. In cells stimulated with PMA, staining with EEA.1 (green) monoclonal antibody followed by the secondary antibody conjugated with FITC was included. Insets on the right of images of vehicle-treated cells and on the bottom-right of PMA-stimulated cells show high magnification of areas marked by white rectangles. Pearson coefficient is shown in the right-low corner of images. Scale bars, 10μM.

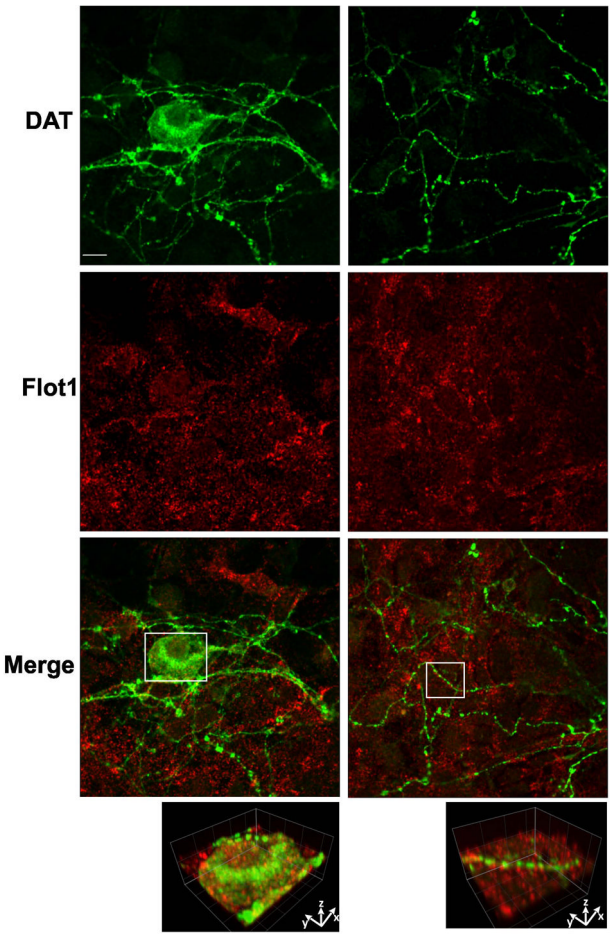

Figure 7. Comparison of localization of flotillin-1 and DAT in dopaminergic neurons

Primary mesencephalic postnatal cultures were fixed, permeabilized and stained with rat monoclonal antibody to DAT (green) and rabbit monoclonal antibody to flotillin-1 (red) followed by secondary to rat and rabbit labeled with Alexa488 and Cy5, respectively. Left column, soma and proximal processes. Right column, distal processes. Insets below show high magnification 3-D volume view of areas marked by white rectangles. Scale bars, 10 μM.

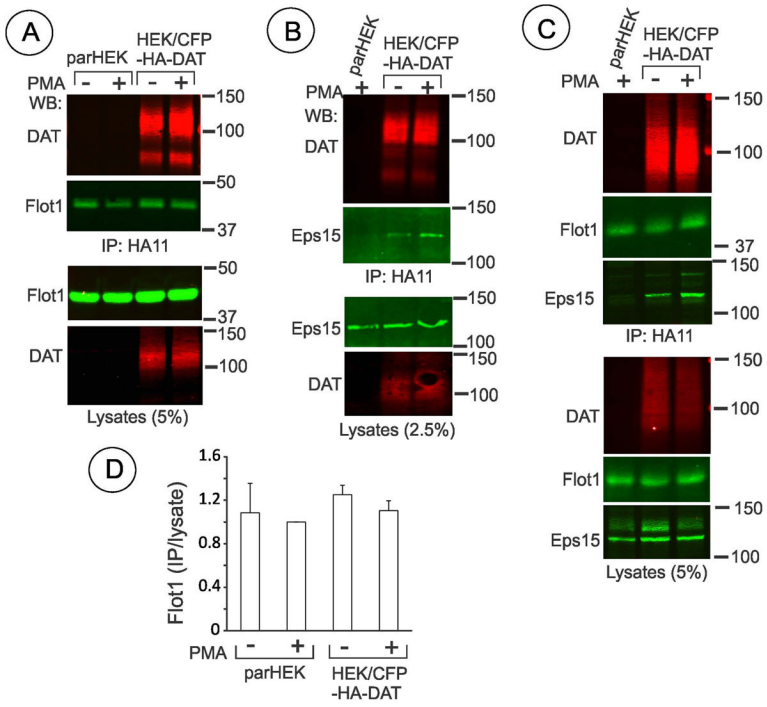

Figure 8. Co-immunoprecipitation of DAT with flotillin-1 and Eps15

(**A, B and C**) Parental HEK293 and HEK/CFP-HA-DAT cells were treated with 1 μM PMA or DMSO for 30 min (***A***) and or 15 min(***B*** and **C**), lysed in TGH (***A and B***) or IGH (***C***), and CFP-HA-DAT was precipitated with the HA11 antibody. Following electrophoresis and transfer, CFP-HA-DAT immunoprecipitates and aliquots of lysates were probed with antibodies to flotillin-1, DAT and Eps15.

(**D**) Quantification of six experiments exemplified in (***A***) and (***C***). Bars represent the mean amounts (+/−S.E.) of co-immunoprecipitated flotillin-1 normalized to the total amount of flotillin-1 in lysates (arbitrary units). In each experiment the ratio of immunoprecipitated/ total flotillin-1 is further normalized to that in parHEK293 treated with PMA.

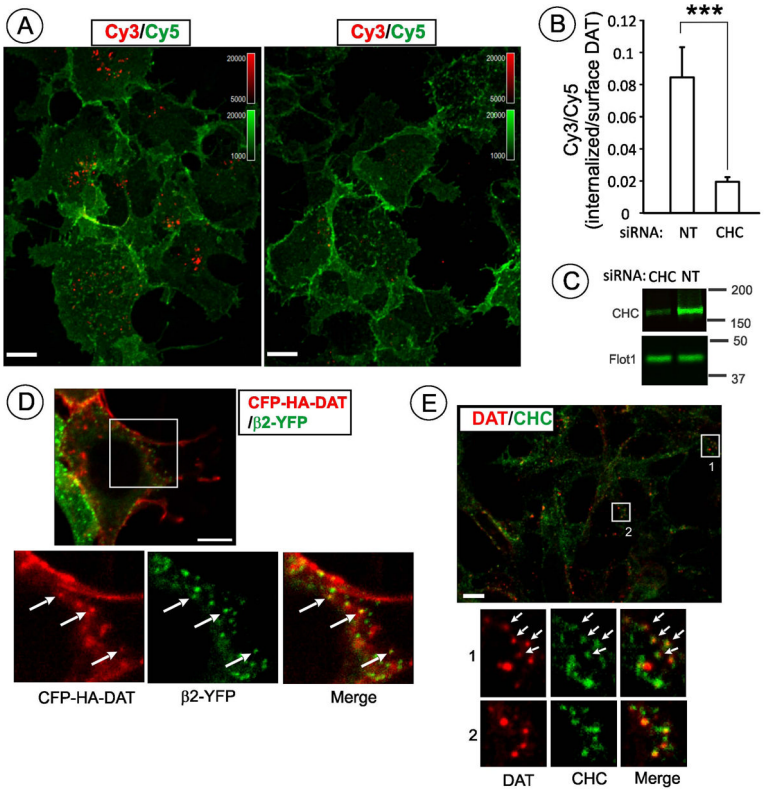

Figure 9. PMA-dependent endocytosis of DAT in HEK293 cells is clathrin-dependent

(**A**) HEK/CFP-HA-DAT cells transfected with non-targeting siRNA (***NT***) or CHC siRNA were incubated with 1 μM PMA or DMSO (***veh***) for 30 min. HA11 internalization assay was performed as described in "Methods". Single confocal sections of merged 3D-images of Cy5 immunofluorescence (green, surface CFP-HA-DAT) and Cy3 immunofluorescence (red, internalized CFP-HA-DAT) are presented. Identical intensityscales are used. Scale bars, 10 μM.

(**B**) Quantification of several experiments performed identically to the experiment presented in (***A***). Bars represent mean values (+/−S.E.) of internalized/surface ratio of HA11-DAT fluorescence normalized to this ratio in control (NT) cells treated with PMA. n=10. ***P<0.005.

(**C**) Western blot detection of CHC in cells treated as in (***A)***. Total cell lysates were blotted with antibodies to CHC and flotillin-1 (loading control).

(**D**) HEK/CFP-HA-DAT cells transfected with AP-2 subunitβ2-YFPwere incubated with 1 μM PMA for 15 min and fixed. Single confocal section is shown. Insets represent high magnification of areas marked by white rectangle (sum projection of 3D stack of 5 confocal images). Additionally, co-localized CFP-HA-DAT and AP-2 dots are indicated by arrows. Scale bar, 10 μM.

(**E**) HEK/DAT cells were stimulated with 1 μM PMA for 15 min and fixed, followed by sequential staining with rat monoclonal antibody to DAT (red) and then mouse monoclonal antibody to clathrin (X22) (green). Insets represent high magnification of areas marked by white rectangle. Additionally, co-localized DAT and clathrin dots are indicated by arrows. Scale bar, 10 μM.

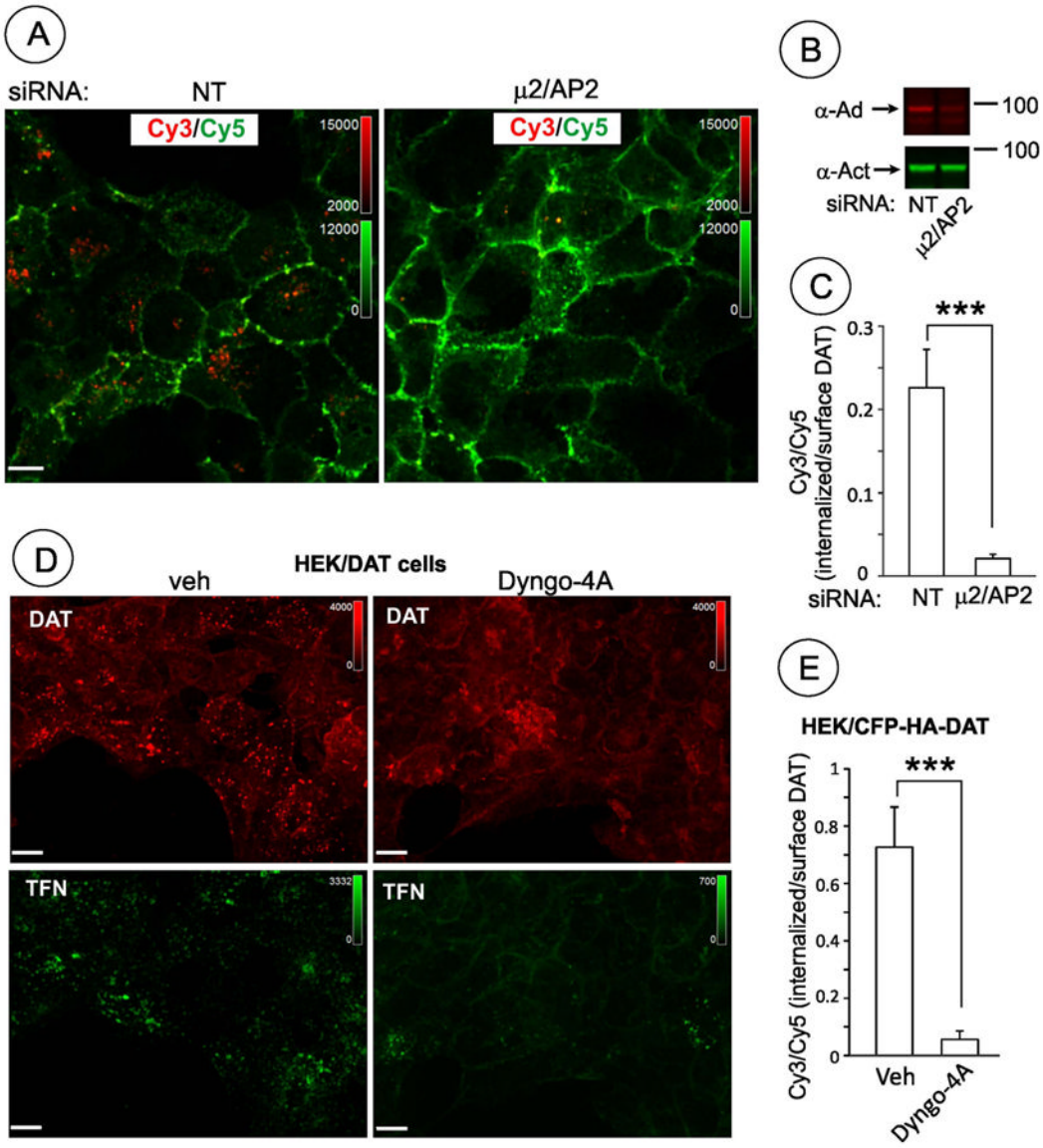

Figure 10. PMA-dependent endocytosis of DAT in HEK293 cells is AP-2-and dynamin-dependent

(**A**) HEK/CFP-HA-DAT cells transfected with non-targeting siRNA (***NT***) or μ2/AP-2 siRNA were incubated with 1 μM PMA or DMSO (***veh***) for 30 min. HA11 endocytosis assay was performed as described in "Methods". Single confocal images of merged 3D-images of Cy5 immunofluorescence (green, surface CFP-HA-DAT) and Cy3 immunofluorescence (red, internalized CFP-HA-DAT) are presented. Intensity scales are shown. Scale bars, 10 μM.

(**B**) Quantification of the experiments presented in (***A***). Bars represent mean values (+/−S.E.) of internalized/surface ratio of HA11-DAT fluorescence. n=10. ***P<0.001.

(**C**) Western blot detection of AP-2 in cells treated as in (***A)***. Total cell lysates were blotted with monoclonal anti-α-adaptin AC.1-M11 (α-Ad) and α-actinin (α-Act, loading control) antibodies.

(**D**) HEK/DAT cells were pre-incubated with serum-free medium for 2 hrs and then 30 min in the same medlum with 30 μM Dyngo-4A or vehicle (DMSO). Cells were then treated

with 1 μM PMA for 30 min in the presence of transferrin-Alexa 488 (TFN, 5 μg/ml) and Dyngo-4A or vehicle in KRH buffer. Transferrin is constitutively endocytosed through clathrin coated pit pathway and used in these experiments as a positive control of Dyngo-4A effects. The cells were fixed, permeabilized and stained with rat monoclonal antibody to DAT (MAB369) followed by cy3-labeled secondary. Representative images (single confocal sections) of 3D stack of confocal images are shown. Scale bars, 10 μM.
(**E**) HEK/CFP-HA-DAT cells treated with Dyngo-4A as described in (D) were incubated with 1 μM PMA for 30 min. HA11 internalization assay was performed and the Cy3/Cy5 ratios quantified as described in “Methods”. Bars represent mean values (+/−S.E.) of internalized/surface ratio of HA11-DAT fluorescence. n=10. ***P<0.005.

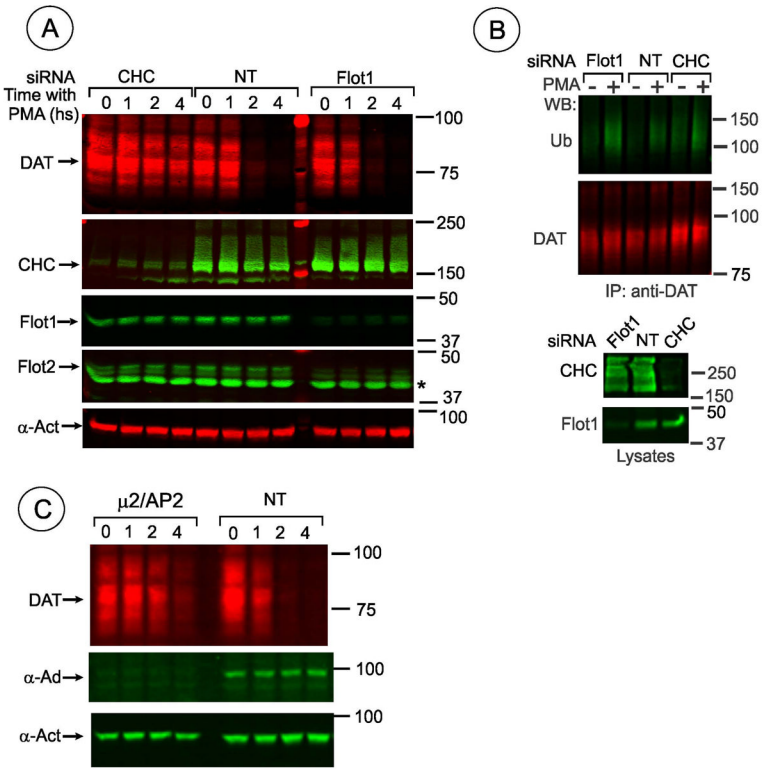

Figure 11. PMA-induced down-regulation of DAT in HEK293 cells is blocked by clathrin but not affected by flotillin knockdowns

(**A**) HEK/DAT cells transfected with control (NT), flotillin-1 (Flot-1) or clathrin heavy chain (CHC) siRNAs were incubated with 50 μg/ml CHX for 2 hrs to inhibit protein synthesis before incubation with PMA (1μM) for indicated times. The cells were lysed and the lysates were probed with rat monoclonal DAT, rabbit monoclonal flotilin-1, rabbit polyclonal flotilin-2 (asterisk marks 40 KDa protein non-specifically recognized by a particular batch of antibodies), CHC and α-actinin (loading control) antibodies. The average efficiency of flotillin-1 knockdown was 75.5%.

(B) HEK/DAT cells transfected with non-targeting siRNA (***NT***), D6targeting human flotillin-1 or CHC siRNA were treated with 1 μM PMA or DMSO for 30 min, lysed in TGH, and DAT was precipitated with the rat monoclonal antibody (MAB369). Following electrophoresis and transfer, DAT immunoprecipitates were probed with antibodies to ubiquitin and DAT. Aliquots of lysates (20%) were blotted with flotillin-1 and CHC antibodies.

(**C**) HEK/DAT cells transfected with control (NT) or μ2/AP-2 siRNAs were incubated with CHX and PMA as in (***A***). The cells were lysed and the lysates were probed with rat monoclonal DAT, mouse monoclonal anti-α-adaptin AC1 (α-Ad) and and rabbit polyclonal α-actinin (α-Act, loading control) antibodies.